



NEAMS Spring meeting INL LLS work on high burnup

May 2021

Changing the World's Energy Future

Larry K Aagesen Jr, Wen Jiang, Sudipta Biswas



INL is a U.S. Department of Energy National Laboratory operated by Battelle Energy Alliance, LLC

DISCLAIMER

This information was prepared as an account of work sponsored by an agency of the U.S. Government. Neither the U.S. Government nor any agency thereof, nor any of their employees, makes any warranty, expressed or implied, or assumes any legal liability or responsibility for the accuracy, completeness, or usefulness, of any information, apparatus, product, or process disclosed, or represents that its use would not infringe privately owned rights. References herein to any specific commercial product, process, or service by trade name, trade mark, manufacturer, or otherwise, does not necessarily constitute or imply its endorsement, recommendation, or favoring by the U.S. Government or any agency thereof. The views and opinions of authors expressed herein do not necessarily state or reflect those of the U.S. Government or any agency thereof.

NEAMS Spring meeting INL LLS work on high burnup

Larry K Aagesen Jr, Wen Jiang, Sudipta Biswas

May 2021

**Idaho National Laboratory
Idaho Falls, Idaho 83415**

<http://www.inl.gov>

**Prepared for the
U.S. Department of Energy
Under DOE Idaho Operations Office
Contract DE-AC07-05ID14517**

High Burnup Structure Formation and Gas Bubble Evolution Modeling

Objective:

- Understand mechanisms of HBS formation and associated bubble growth
- Provide microstructure as input for fracture simulations
- Provide pressure input for determining fragmentation criteria

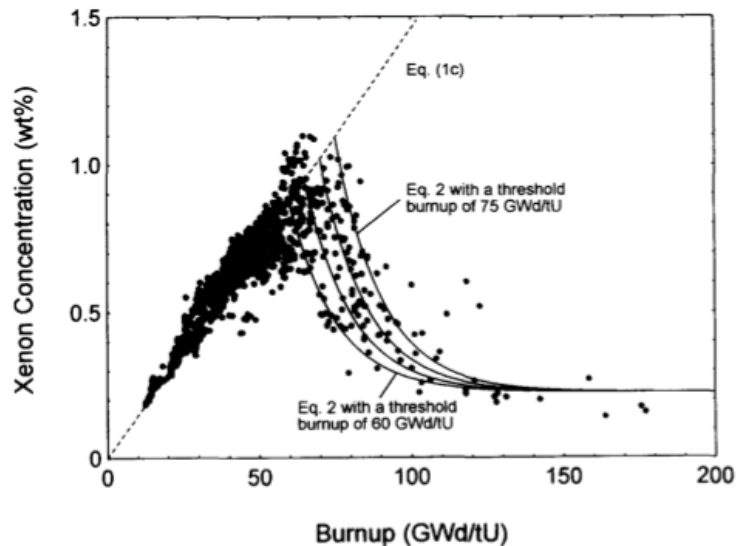
Developments:

- Multi-phase multi-order parameter model capable of capturing arbitrary number of phase, grains, and chemical components
- Model is parameterized with LLS defect evolution data obtained from cluster dynamics simulations
- Pressure calculation has been added to the model
- Established collaboration with AFC experiments for model validation

Model Improvements

- Defect source term and diffusivities updated for operating conditions
- Vacancy sink is added to the model
- Initial super saturation value in the matrix is set based on the experimental data
- Pressure calculation has been added to the model

Van der Waals EOS:
$$P_g = \frac{c_g k_B T}{\Omega - c_g b}$$



Lassman et al., JNM (1995)

Xe Diffusion

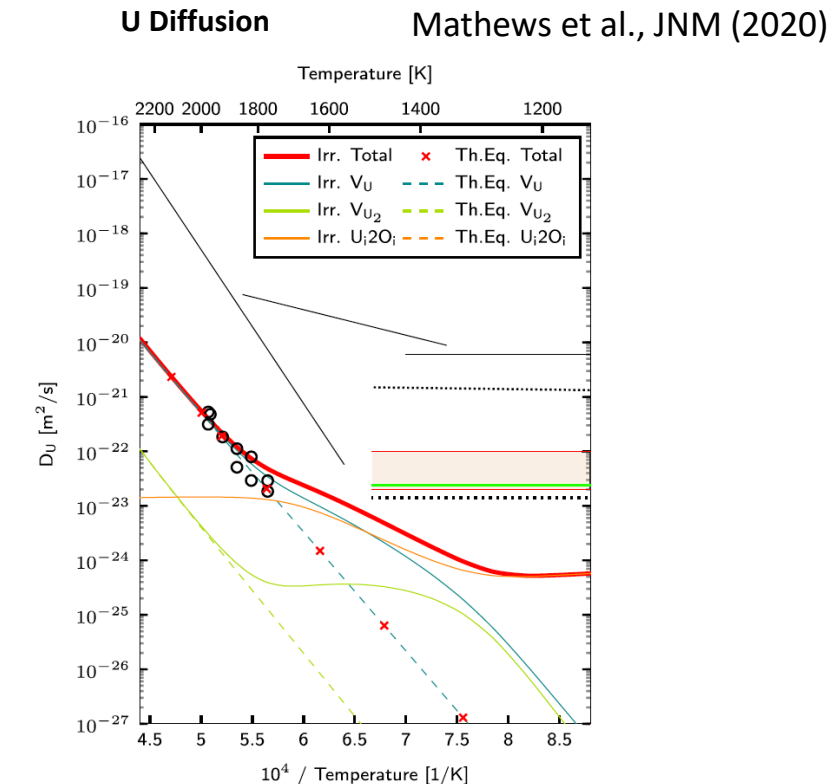
$$D_{tot}(T, \dot{F}) = D_1(T) + D_2(T, \dot{F}) + D_3(\dot{F}),$$

$$D_1(T) = \frac{2.22 \cdot 10^{-7} \exp(-3.26/k_B T)}{1 + 29.0 \exp(-1.84/k_B T)},$$

$$D_2(T, \dot{F}) = 2.82 \cdot 10^{-22} \exp(-2.0 / k_B T) \sqrt{\dot{F}},$$

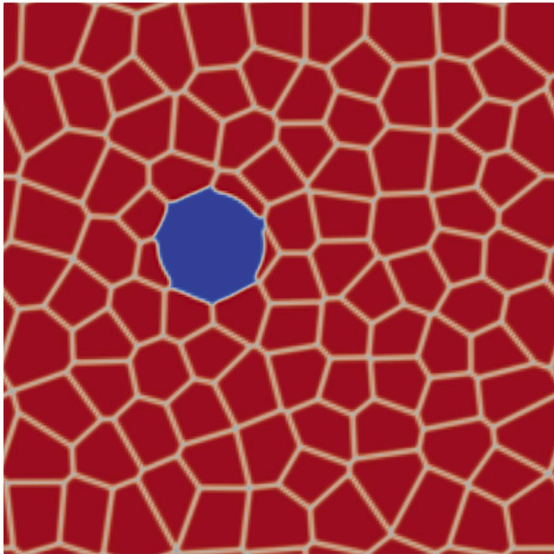
$$D_3(\dot{F}) = 8.5 \cdot 10^{-40} \dot{F},$$

Perriot et al, JNM (2019)

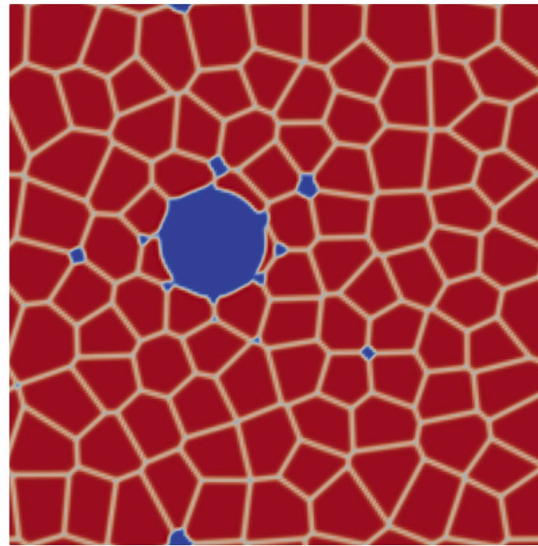


Simulation Results

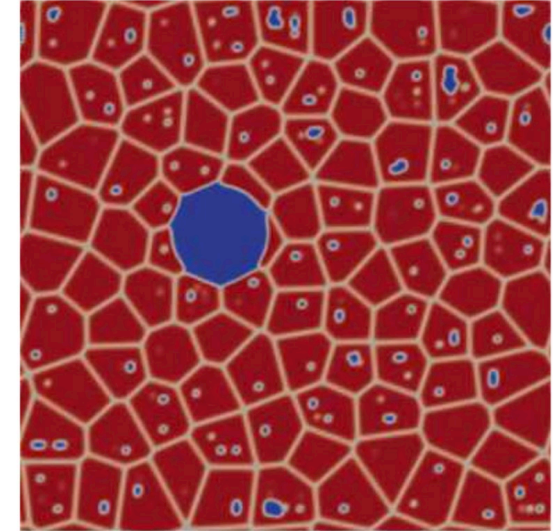
- Competition between the vacancy diffusion and gas diffusion dictates the bubble growth vs. pressure buildup
- Preliminary pressure estimation indicates bubble pressure could go beyond the theoretical value obtained using dislocation punching criteria, verification of the pressure calculation is required



Growth of existing
bubbles



Concurrent Bubble
Formation and Growth

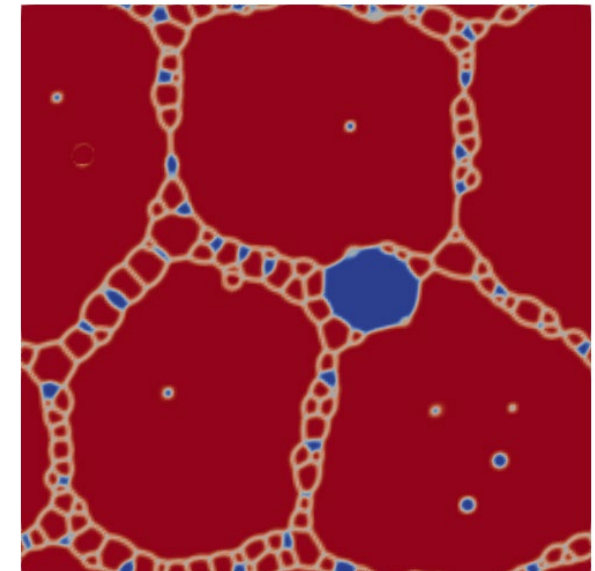
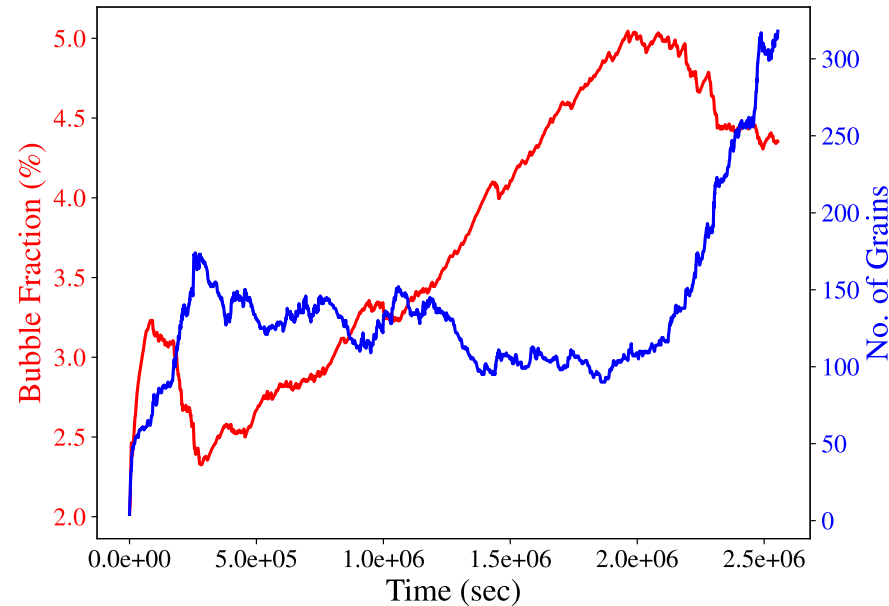
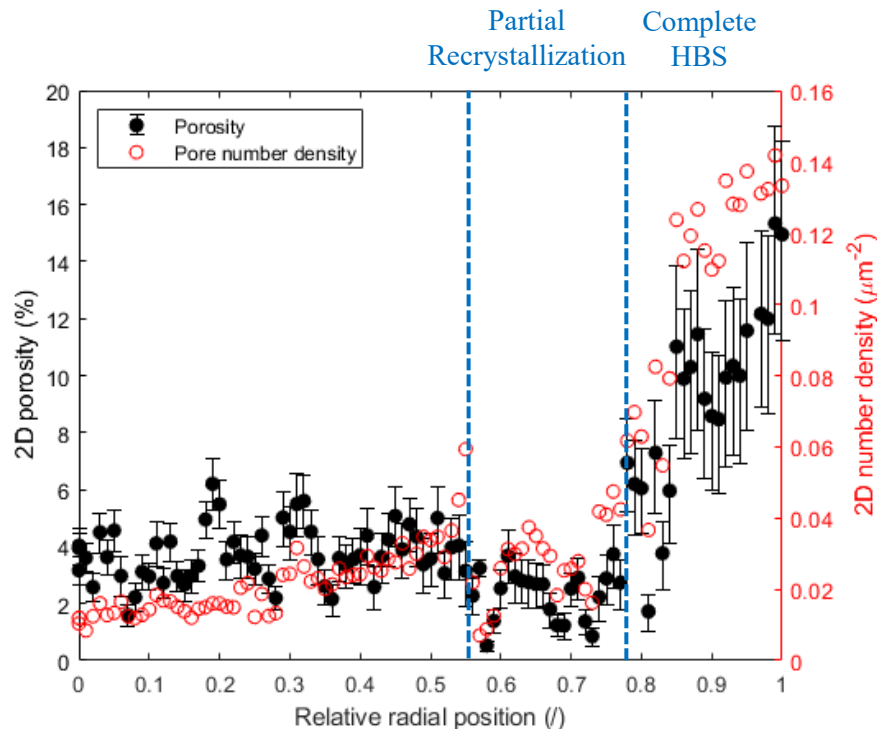
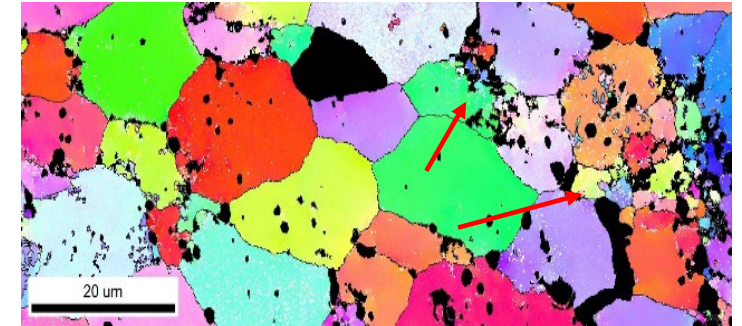


Formation of intra-
granular bubbles

Model Validation

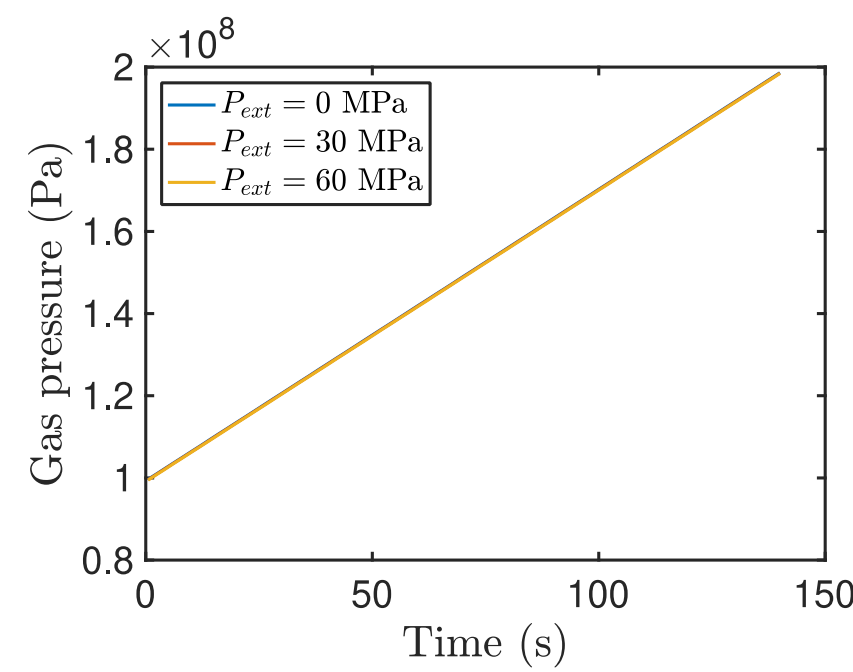
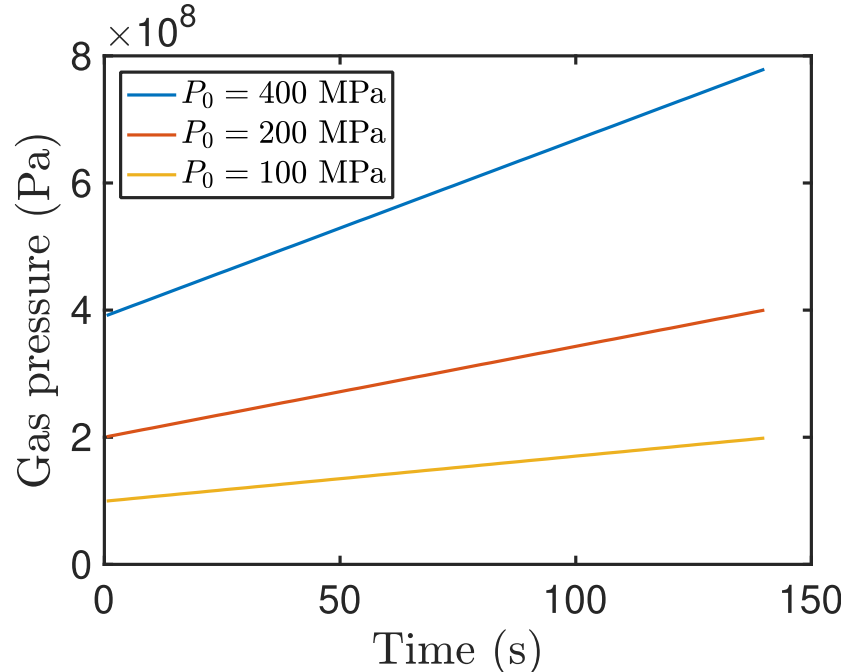
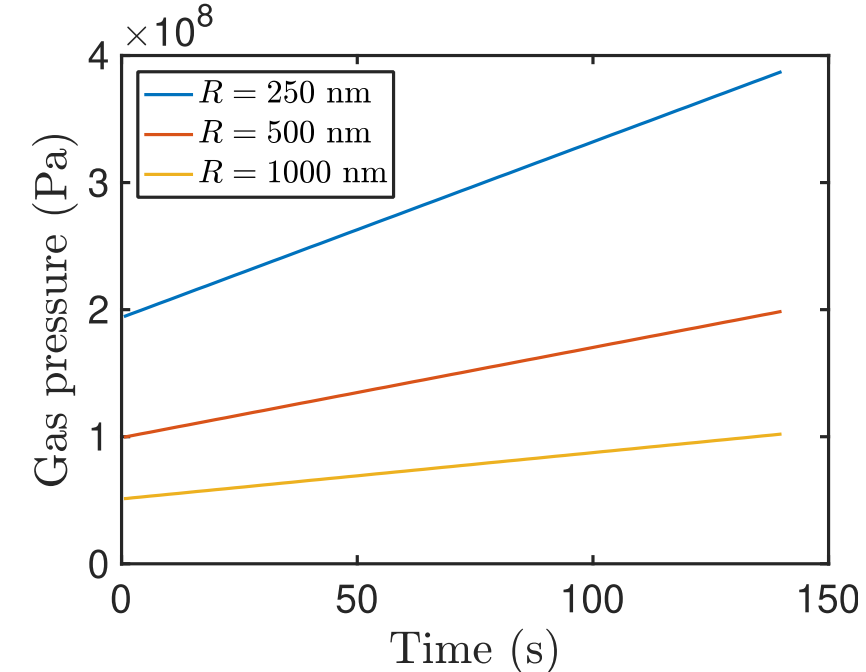
- Simulated microstructure closely resembles the experimentally observed recrystallized microstructures
- Porosity reduction in partially recrystallized zone is also observed experimentally

Experiment Credits: Fabiola Cappia

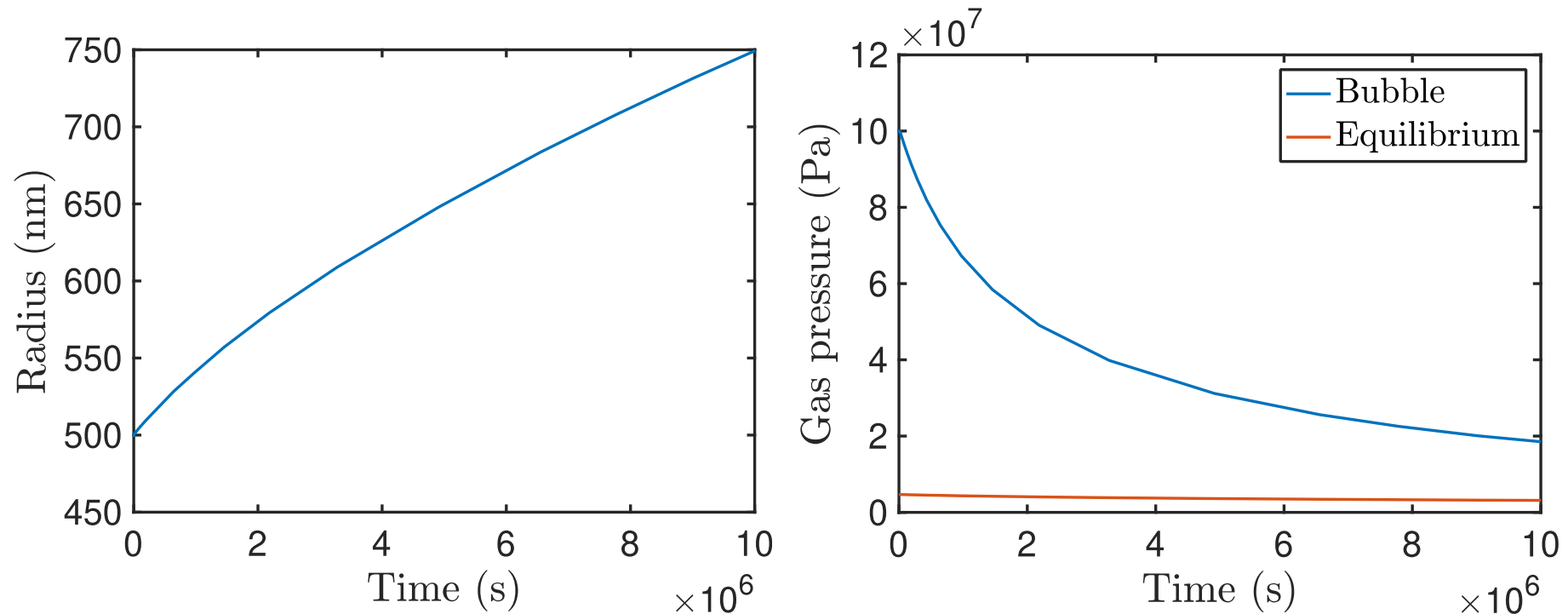


Recap: HBS Bubble response to LOCA transient

- Developed of new phase-field model to address LOCA behavior:
 - KKS formulation (removes bulk contribution to interfacial energy)
 - Includes surface tension of bubble-matrix interface and gas pressure; allows consideration of effect of overpressurized bubbles
- LOCA transients: variations in bubble size, initial pressure, porosity, external pressure
- **Bubble size does not change significantly for any cases considered**
- **Pressure as a function of time passed to PF fracture model**



Bubble growth during steady-state operation

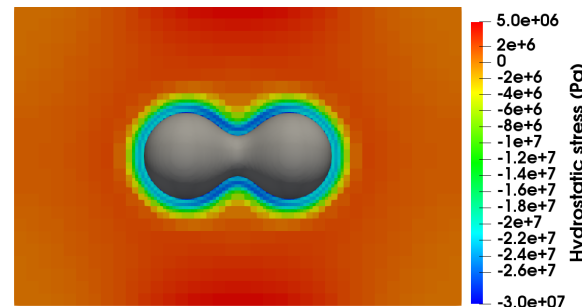


- Assume bubble pressure is 100 MPa in initial conditions
 - Upper bound based on dislocation punching pressure
- Bubble pressure decreases during growth but remains well above equilibrium pressure
 - Increased likelihood of fragmentation during LOCA

Bubble growth during steady-state operation



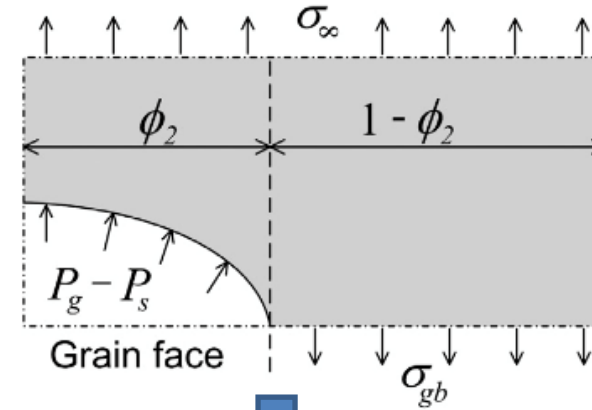
- 3D simulation to 1.5×10^7 s, 2 bubble impingement, initial radii of 300 nm
- Hydrostatic stress surrounding bubbles
 - Region of enhanced compressive hydrostatic stress in “neck”
- **Results of steady state growth and LOCA response incorporated into manuscript submitted to JNM**



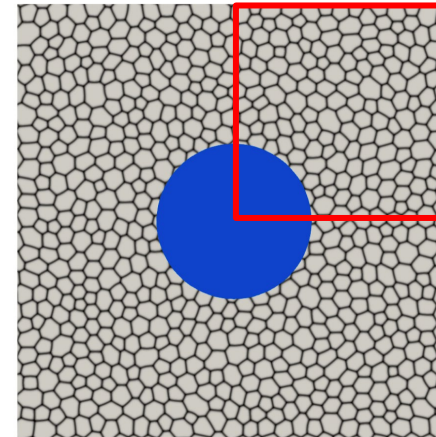
$$t = 1.3 \times 10^6 \text{ s}$$

Development of Physics-Based Criterion for Pulverization for BISON

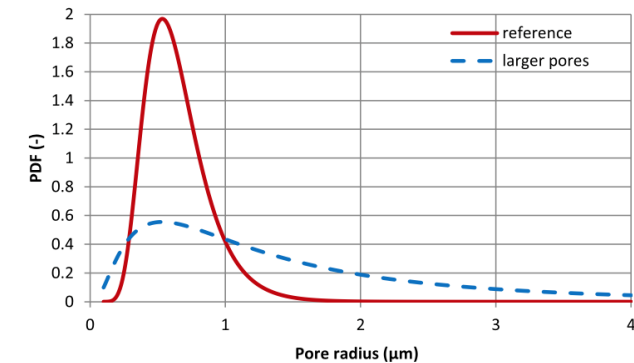
- Began implementation of pulverization based on analytical expression (Olander)
 - (To be supplanted by Phase-Field Fracture results)
- Originally developed for lenticular (non-HBS) bubbles
 - Adapted to HBS geometry using porosity, assume worst-case scenario of flat GB
- Pulverization occurs when $P_g > P_g^{cr}$
- Determine P_g during transient for most frequently occurring bubble, $R = 0.53 \mu\text{m}$
 - Initial pressure $\sim 100 \text{ MPa}$ at 673K based on experimental data
 - (To be supplanted by results from Phase-Field HBS formation model)



$$P_g^{cr} = P_s + \frac{\sigma_{gb}^{cr}(1 - \phi_2) - \sigma_\infty}{\phi_2}.$$



Determine ϕ_2 from porosity (empirical)



Kulacsy, JNM 466, 409-416 (2015)

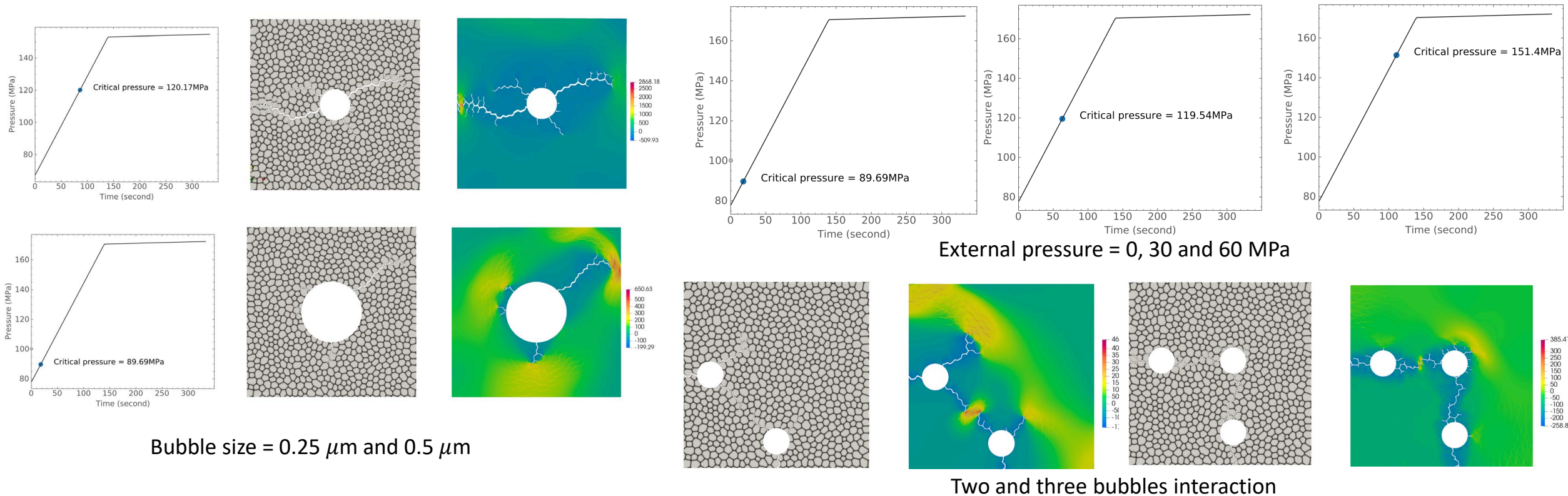
Phase-field fragmentation modeling

Developed a phase-field model for quasi-brittle pressurized fracture

- It remains elastic behavior before crack initiates
- Critical fracture strength is independent of length-scale parameter
- It can predict general softening laws

Phase-field fracture model was used to study HBS fragmentation behaviors

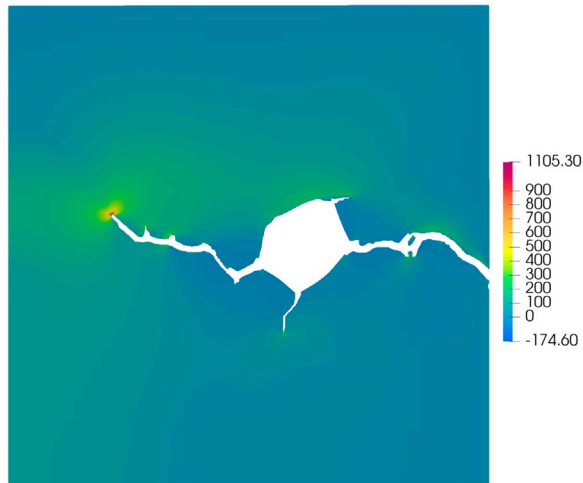
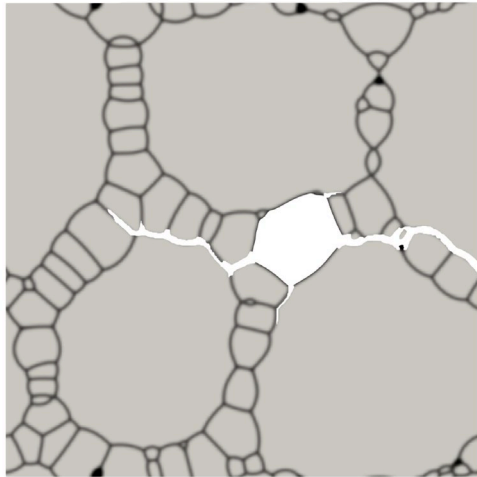
- Effect of bubble sizes: critical pressure is lower for the larger bubble
- Effect of external pressure: critical pressure becomes higher for larger external pressure values
- Effect of bubble interaction: fragmentation size is likely determined by bubble spatial distribution



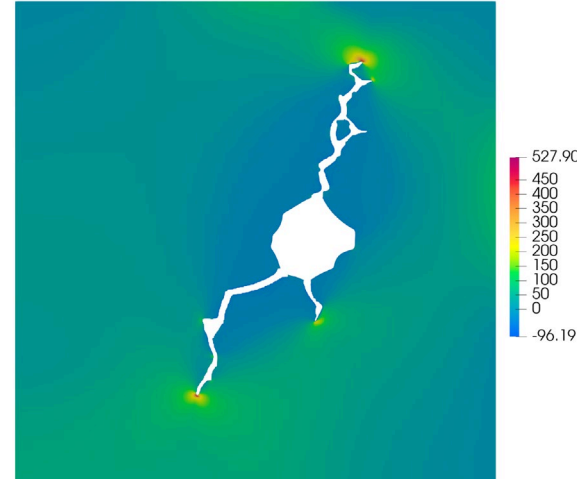
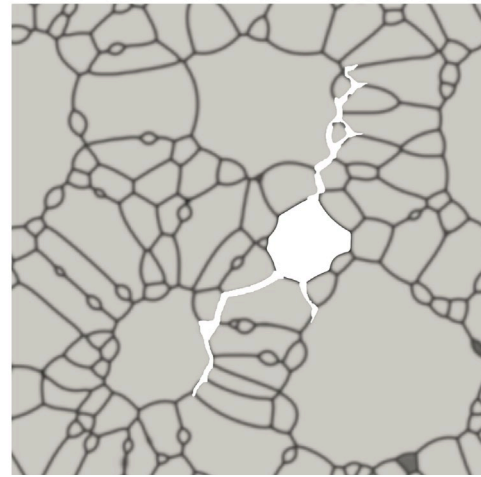
Fragmentation in partial HBS

Phase-field fracture model was used to simulate fragmentation behaviors of partial HBS

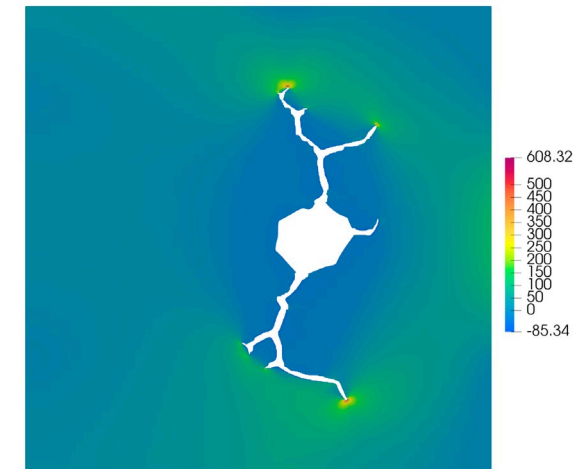
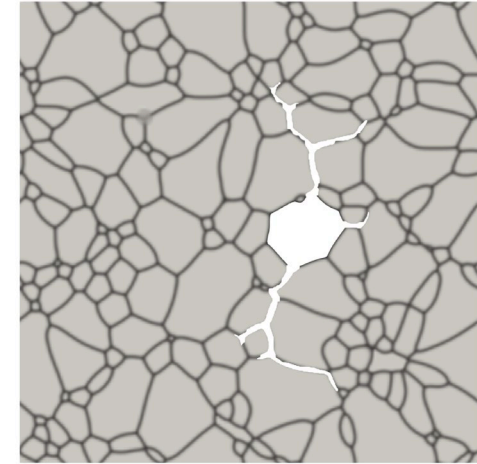
- Use the output from the HBS formation simulations as our initial condition
- Three HBS at different recrystallization stages with 25%, 60% and 100% recrystallization fraction were considered
- Crack initiation locations and crack propagation paths varied among the three cases because recrystallized grain structures change.



25 % recrystallization stage



60 % recrystallization stage

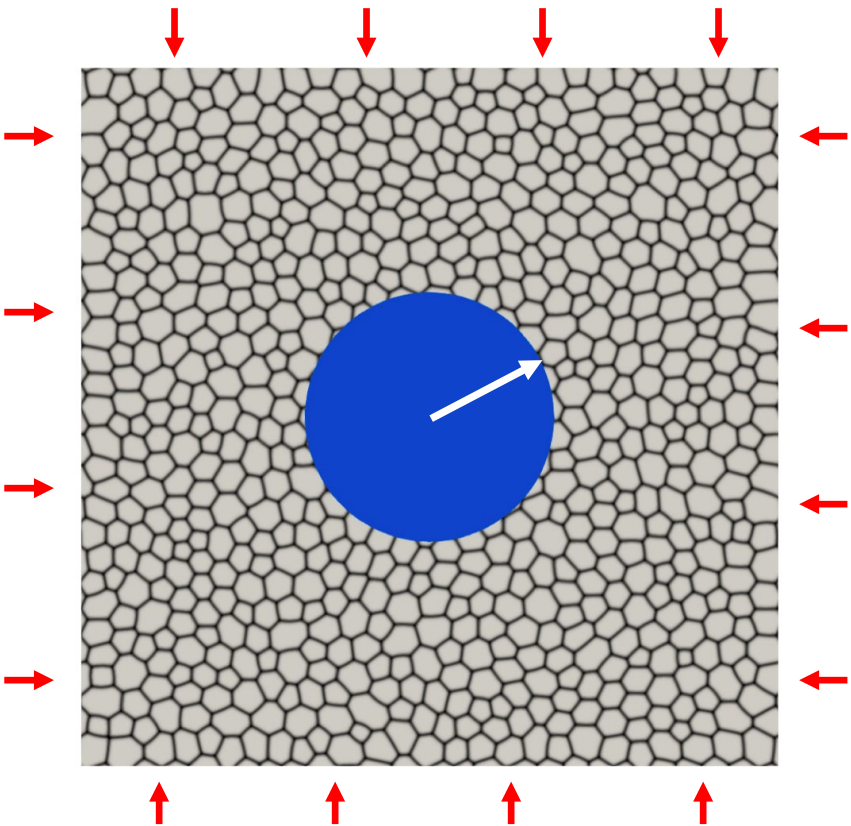


100 % recrystallization stage

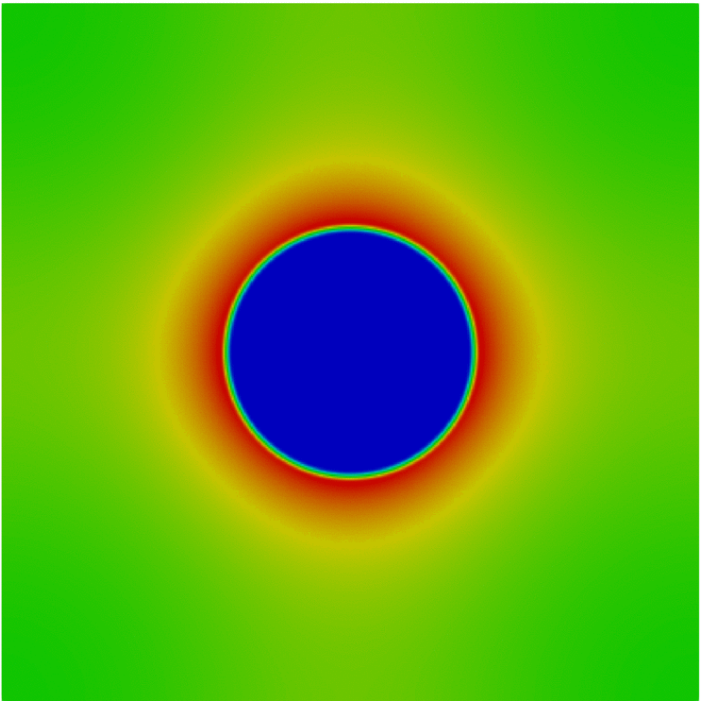
Determine BISON fragmentation criterion

Phase-field fracture model was used to inform fragmentation criterion for BISON models

- Use periodic boundary conditions to get more realistic simulation results.
- Consider bubble size, bubble distance and external pressures



| External pressure (MPa) | 0 | 10 | 20 | 30 | 40 | 50 | 60 |
|--------------------------------|-----|-----|-----|-----|-----|-----|-----|
| Critical bubble pressure (MPa) | 112 | 124 | 132 | 144 | 152 | 164 | 176 |



Incorporate elastic-plastic anisotropy

Developed crystal plasticity based phase field fracture model

- Derived variational consistent crystal plasticity based phase-field fracture model
- Implemented a new generic phase field damage model that uses crystal plasticity constitutive laws
- Anisotropic elastic-plastic deformation due to grain orientations
- crack driving forces include elastic and plastic contributions.

Constitutive relations (consistent viscoplasticity)

$$\text{stress-strain relation: } \mathbf{P} = g^e \mathbf{F}^e \mathbf{S}^e \mathbf{F}^{p^{-T}}, \quad \mathbf{S}^e = \mathbb{C} : \mathbf{E}^e,$$

$$\text{plastic hardening: } Y_\alpha^{\text{en}} = g^p \left[\tau_c^\alpha + \tau_0 \gamma_{,\gamma_\alpha} \left(\frac{\gamma}{\gamma_0} \right)^{1/n} \right], \quad Y_\alpha^{\text{dis}} = g^p \tau_c^\alpha \left(\frac{\dot{\gamma}^\alpha}{\dot{\gamma}_0} \right)^{1/m},$$

$$\text{micro-forces: } f^{\text{en}} = \frac{2\mathcal{G}_c}{\pi l} (1-d) + \psi_{,d}^e + e_\alpha \psi_{\alpha,d}^p, \quad f^{\text{dis}} = \eta \dot{d}, \quad \xi = \frac{2\mathcal{G}_c l}{\pi} \nabla d.$$

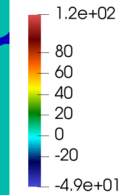
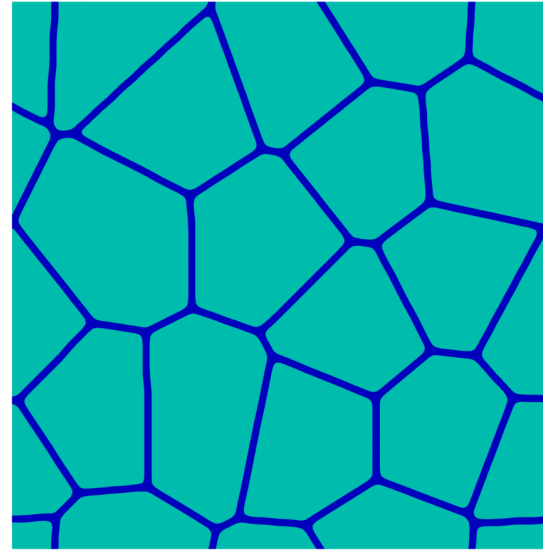
or by the constitutive relations (for the Perzyna viscoplasticity model):

Constitutive relations (Perzyna viscoplasticity)

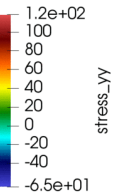
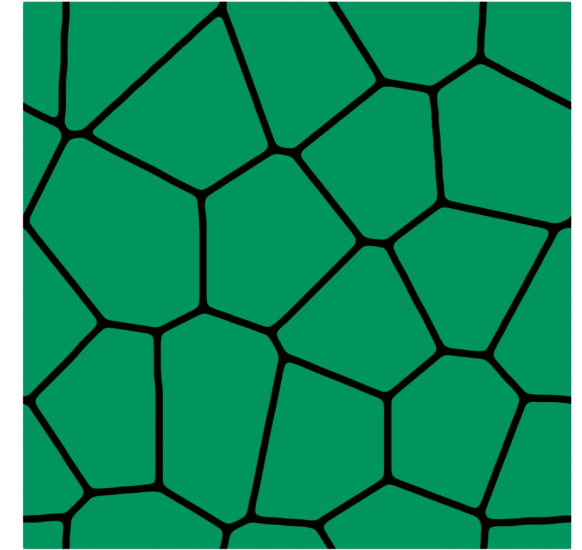
$$\text{stress-strain relation: } \mathbf{P} = g^e \mathbf{F}^e \mathbf{S}^e \mathbf{F}^{p^{-T}}, \quad \mathbf{S}^e = \mathbb{C} : \mathbf{E}^e,$$

$$\text{plastic hardening: } Y_\alpha^{\text{en}} = 0, \quad Y_\alpha^{\text{dis}} = \tau_\alpha, \quad \dot{\gamma}_\alpha = g^p \left| \frac{\tau_\alpha}{\tau_c^\alpha + k_0/\sqrt{s}} \right|^{1/m} \text{sgn}(\tau_\alpha) \dot{\gamma}_0,$$

$$\text{micro-forces: } f^{\text{en}} = \frac{2\mathcal{G}_c}{\pi l} (1-d) + \psi_{,d}^e, \quad f^{\text{dis}} = \eta \dot{d}, \quad \xi = \frac{2\mathcal{G}_c l}{\pi} \nabla d.$$



Transgranular fracture



Intergranular fracture